DOI: 10.1002/ejic.200700775

# Direct Synthesis of Zr-Containing Hybrid Periodic Mesoporous Organosilicas with Tunable Zirconium Content

**Shang-Ru Zhai,[a] Sung Soo Park,[a] Mina Park,[a] M. Habib Ullah,[a] and Chang-Sik Ha*[a]**

**Keywords:** Silicates / Template synthesis / Orangic–inorganic hybrid composites / Mesoporous materials

Highly ordered Zr-containing periodic mesoporous organosilicas (ZrPMO) with different Zr/Si ratios were successfully synthesized, for the first time, by employing a $ZrOCl_2$/NaCl combination as the promoting agent and by simply adjusting the molar ratio of the zirconium species to the organosilica precursor; no addition of mineral acids was necessary. The effect of preparation parameters on the structural and textural properties were carefully investigated by using different ratios of NaCl/Si and Zr/Si. It was found that both salts are essential for this system and highly ordered ZrPMOs can be prepared within fairly wide Si/Zr ratios (5–100) while keeping the NaCl/Si ratio constant. To prove the effectiveness of this synthetic pathway with a higher Zr incorporation, ZrPMO materials were also synthesized under strongly acidic conditions for the purpose of comparison. The synthesized ZrPMO materials were thoroughly characterized by ICP-AES, SAXS, $N_2$ sorption, TEM, SEM, $^{13}C$ CP/$^{29}Si$ MAS NMR spectroscopy, XPS, and TGA. Elemental analyses show that the amount of Zr incorporated into ZrPMO, which was synthesized under mild conditions, is greater than that obtained in a strongly acidic environment, and the Zr content, with a Si/Zr ratio up to 12, is close to that in the initial gel composition. A plausible assembly mechanism based on the synergistic effect of both "nonhydrolyzable" (NaCl) and "hydrolyzable" ($ZrOCl_2$) inorganic salts was discussed in detail, where the "salting out" effect and self-generated acidity from both inorganic salts, respectively, are believed to be key factors for the formation of ordered SBA-15-type ZrPMO materials under the synthetic conditions.



## Introduction

Since its first synthesis in 1999,[1–3] periodic mesoporous organosilica (PMO) materials have attracted increasing research attention in the field of ordered mesoporous materials. These novel hybrid materials, characterized with the high organic content incorporated within the framework, were synthesized by the hydrolysis and condensation of bis(trialkoxysilyl)alkylsilanes such as $(R'O)_3Si\text{-}R\text{–}Si(R'O)_3$ with the aid of structure-directing agents.[1–4] The fascinating properties featured by these materials include highly ordered structures and uniform pore-size distributions within a framework formed by a homogeneous distribution of organic fragments and inorganic oxide. In comparison with their inorganic counterparts, these hybrid mesostructures offer unique advantages and enormous possibilities that are closely associated with the characteristics of the organic polymers, such as tunable interfacial and physicochemical properties, by simply varying the organic bridging groups embedded within the mesoporous framework. With the aforementioned advantages, PMO materials are promising candidates in the fields of catalysis, selective adsorption, chromatography, low-*k* devices, or host–guest chemistry.

At present, PMO materials with various framework bridging groups ranging from small aliphatic spacers to aromatic and large heterocyclic ones were successfully synthesized.[5–15] Recently, the synthesis of bi- and multifunctional PMOs has become a hot research topic in this field, because proper selection of these groups allows one to design functional nanocomposites for specific catalytic and environmental applications.[16–21] The synthesis of these materials has been carried out by using cationic, anionic, and nonionic oligomeric and copolymeric surfactants under basic or acidic conditions.

Although the development of PMOs has opened new opportunities in the field of mesoporous materials, there is still a lack of application of these materials to the field of catalysis. Thus, unlike in the case of inorganic mesostructured materials upon which many different heteroatoms have been supported in the hope to discover catalytic properties, only a few examples have been reported on the functionalization of PMOs with the use of heterometallic atoms. Most of them use the organic functionality as a ligand to bind the

[a] National Research Laboratory of Nano-Information Materials, Department of Polymer Science and Engineering, Pusan National University,
Pusan 609-735, Korea
Fax: +82-51-514-4331
E-mail: csha@pusan.ac.kr

Supporting information for this article is available on the WWW under http://www.eurjic.org or from the author.

   

metallic atoms,[22,23] but these procedures are only appropriate for a small amount of metal atom–organic functionality pairs. The second strategy used for synthesizing these metal-functionalized PMOs involves direct synthetic procedures through the isomorphic substitution of the silicon atoms by the metal species of interest. In most cases, however, this procedure has only successfully been applied to the heterogenization of limited metal species in the synthesis of hexagonally packed PMO materials by using cationic surfactants.[24–32] For instance, aluminum was incorporated within the mesoporous framework of ethanesilicas by a direct synthetic method with the use of cationic surfactants under basic conditions.[24–26] The resultant hybrid mesostructures showed a high hydrothermal stability that can be attributed to the presence of hydrophobic ethane bridging groups distributed within the whole framework. Furthermore, this highly hydrophobic character improved the catalytic behavior in alkylation reactions in comparison with that shown by AlMCM-41 materials.[24] Likewise, titanium, chromium, vanadium, and other species have also been incorporated into the structure of ethane-bridged PMO materials, and these obtained materials showed a good degree of incorporation of the metal functionality.[27–33] In these works, it was reported that Ti-containing PMO materials are highly hydrophobic and fairly efficient in the epoxidation of α-pinene,[27] epoxidation of propene into propene oxide in the vapor phase,[28] and ammoxidation of ketones to oximes.[29] Apparently, the enhanced catalytic efficiency was directly associated with the framework hydrophobicity of these hybrid catalysts. Among these limited reports,[24–33] however, only one paper was devoted to the synthesis of SBA-15-type PMO from titanocene dichloride by using copolymeric surfactant under acidic conditions, and these hybrid catalysts showed good performance in the epoxidation of 1-octene with hydroperoxides.[33] Currently, there is a quest for large-pore hybrid PMO materials from the point of view of immobilization or transformation of bulky molecules; therefore, these results have prompted us to take a step forward in the synthesis of metal-functionalized PMO materials with large pore diameters.

In the present study, we report an effective and convenient synthetic pathway to zirconium-functionalized periodic mesoporous organosilicas (PMOs) by employing a $ZrOCl_2$/NaCl combination as the promoting agent under acid-free conditions. This is, to the best of our knowledge, the first example of SBA-15-type ZrPMO with tunable Zr content synthesized by simply adjusting the molar ratio of Zr/Si while retaining another NaCl/Si ratio constant. The resultant materials were characterized and have excellent structural ordering, narrow pore-size distributions, and hybrid organic–inorganic frameworks; meanwhile, these characterization results indicate that both inorganic salts are essential to the formation of ordered ZrPMO materials. More desirably, this novel synthetic system is more advantageous in comparison to the HCl-assisted synthetic pathway either from the point of view of zirconium incorporation or the structural properties of the obtained ZrPMO materials.

## Results and Discussion

### Effect of Both NaCl/Si and Zr/Si Molar Ratios

As reported, since its first synthesis in 1998,[34] SBA-15-type materials have been extensively studied.[35] However, it is difficult to synthesize Zr-incorporated SBA-15 silicas with a high amount of Zr loading, because the Zr–O–Si bonds are easily dissociated; this is due to the hydrolysis of zirconium precursors under the strongly acidic hydrothermal preparation conditions. However, by decreasing the acidity of the synthetic system to balance the hydrolysis rate of Zr precursors with that of the silicon precursors, the interaction between the Zr–OH and Si–OH species in the synthesis gels could be effectively enhanced, which would result in a higher amount of Zr ion incorporated in the framework of SBA-15-type materials. Therefore, by following our previous studies,[7,36] this paper reports an effective direct synthesis of a higher amount of Zr incorporated in the SBA-15-like PMO materials by employing a $ZrOCl_2$/NaCl combination as the promoting agent under acid-free conditions, and the Zr content loaded in the PMO materials is tunable by simply adjusting the Si/Zr molar ratios from 5 to 100 in the synthesis gels while keeping the NaCl/Si ratio constant.

To prove the importance of the salt combination during the synthesis, the effect of both NaCl/Si and Si/Zr ratios were thoroughly investigated. With Si/Zr = 10 for all samples, the variation of the SAXS patterns as a function of the NaCl/Si ratios is illustrated in Figure 1. Well-defined SAXS patterns are clearly observed for those samples synthesized with NaCl/Si ratios varied from 1–6, similar to those recorded for all SBA-15-type materials as described by Zhao et al.[34,35] The SAXS patterns of these samples exhibit at least three well-resolved peaks, which can be indexed to the (100), (110), and (200) reflections of the hexagonal space group *p6mm*. Among these samples, however, the optimal structural ordering of the hexagonal mesostructure was obtained for the sample synthesized with a NaCl content around NaCl/Si = 4, which is evidenced by the reflection intensity that decreased as the NaCl/Si ratios increased or decreased relative to this point. This observation is reminiscent of the previous results for large-pore PMOs, which proved that highly ordered mesostructures were successfully prepared in the presence of a large amount of Na(K)Cl salts.[7,37]

Therefore, the ratio of NaCl/Si was fixed at 4 in the following experiments that allowed the study of the effects of the Si/Zr molar ratios on the synthesis; Figure 2 shows the SAXS patterns of samples synthesized with different Si/Zr ratios varied from 5–100. With only one exception from that prepared without zirconium salt, all other patterns of the extracted PMOs exhibit very sharp reflections, which clearly indicates a high degree of structural ordering. Likewise, the reflections can be indexed as (100), (110), and (200) peaks according to the 2D hexagonal symmetry of the materials.[34] The results strongly reveal the effectiveness of this synthetic method irrespective of the fairly wide range of Zr/Si ratios, which is somewhat similar to the studies

  

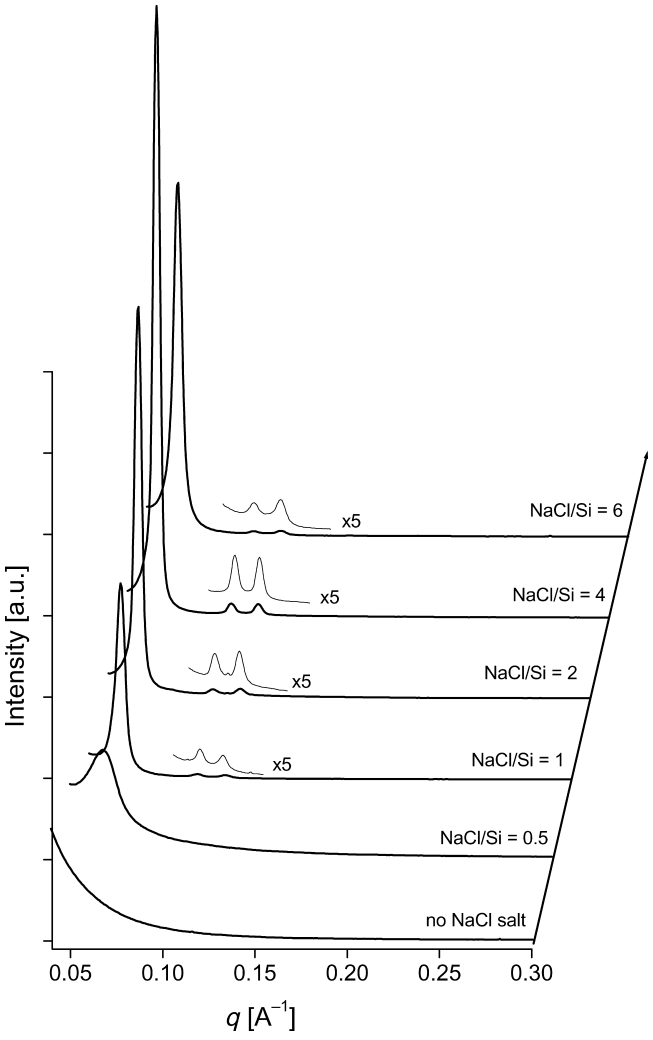


Figure 1. SAXS patterns of samples prepared at different NaCl/Si ratios while keeping Si/Zr = 10.

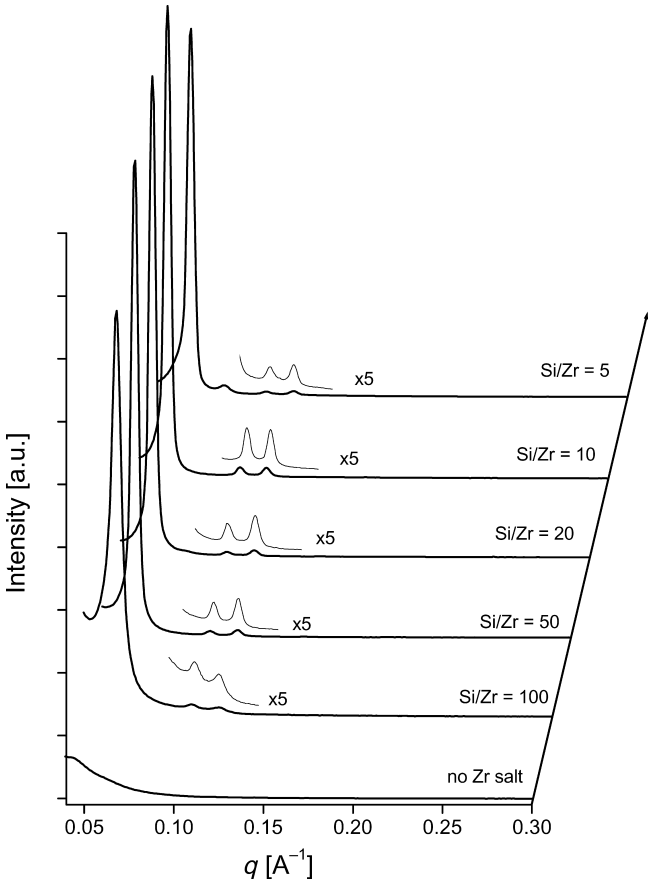


Figure 2. SAXS patterns of materials synthesized by using different Si/Zr molar ratios while fixing NaCl/Si = 4.

reported recently where highly ordered SBA-15-like PMO materials were facilely prepared within a wide composition range by employing a KCl-assisted low-acid-concentration synthetic pathway.[37] By combining the SAXS data (Figures 1 and 2), we can clearly see that the combination of $ZrOCl_2$/NaCl is indispensable for this synthesis, that is, highly ordered PMO materials are easily achievable with a variable zirconium salt amount while keeping the NaCl/Si ratio constant; this fascinating observation has never been reported for large-pore PMO materials templated by block copolymer surfactants.

To further prove the important effect of this salt combination on the structural ordering of the resultant materials, a series of samples were also synthesized by using various acid concentrations for comparison purpose, where the zirconium salt amount with Si/Zr = 10 is constant through all experiments. Figure 3 shows that the samples synthesized with 0.4 and 1.0 M HCl exhibit a single peak together with a broad shoulder and another one from 0.2 M HCl only possesses a very broad peak. Such reflection patterns are often observed for wormhole-like mesostructures, in agreement with our previous results that disordered PMOs were commonly obtained under strong acidic conditions without the assistance of NaCl.[7] In contrast, the fact that a highly ordered sample can be easily synthesized by using the $ZrOCl_2$/NaCl pair without the addition of any mineral acids further indicates that this salt combination is very effective for the assembly of ordered organosilica–surfactant nanocomposites, even though the amount of zirconium salt added in the reaction gels is quite small; a plausible formation mechanism will be discussed below.

The zirconium contents in the PMO materials synthesized by using both salt pair and HCl solutions were determined by ICP-AES and XPS techniques, and the results are summarized in Table 1. The former technique provides the elemental analysis of the bulk sample, whereas the latter gives the surface composition information. The atomic ratios of Si/Zr in the solids synthesized by using $ZrOCl_2$/NaCl were found to be slightly larger than that in the synthesis gels. These results might be due to variations in zirconium leaching during the extraction processes by using acidified ethanol. It was reported that this phenomenon is common to directly synthesized metal-incorporated hybrid frameworks where the complete removal of surfactant is relatively more difficult due to the enhanced interaction between the surfactant and the metal species.[38,39] However, the zirconium content in the above-described materials is consider-

  

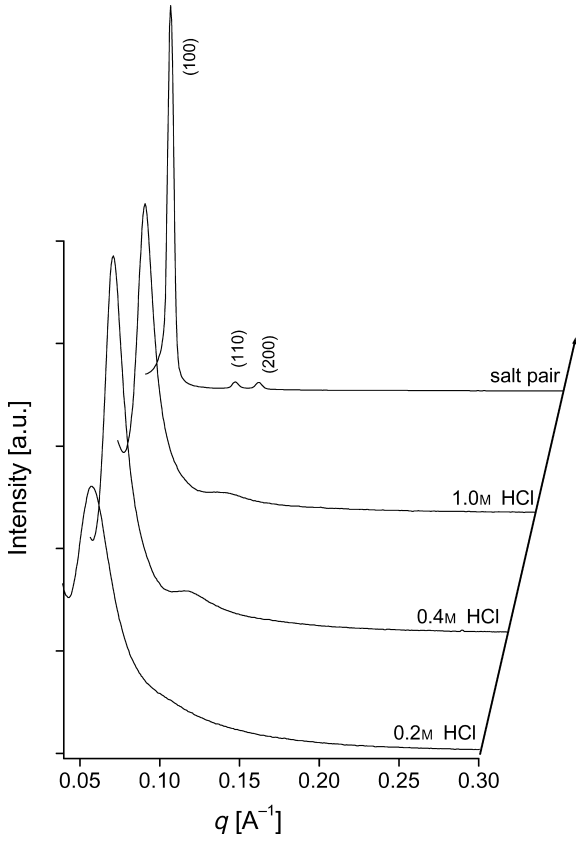


Figure 3. SAXS patterns of PMO materials synthesized by using different HCl concentrations, here the Si/Zr molar ratio is 10 for all samples.

ably higher than that of the samples synthesized with HCl solutions especially for those obtained with 0.4 or 1.0 M HCl, which is in agreement with the reported observations.[39] Noticeably, this synthetic pathway, that is, the use of $ZrOCl_2$/NaCl as the promoting agent, is not only more effective for the formation of highly ordered PMO materials but also more favorable for zirconium incorporation than the HCl-assisted synthesis, which can be considered the main advantage of this route.

In addition, the surface Si/Zr atomic ratios are, for representative materials synthesized from the $ZrOCl_2$–NaCl pair, significantly larger than that used in the synthesis (see Table 1). This is expected by taking into account that zirconium species may be mainly incorporated into the hybrid frameworks, and consequently, zirconium atoms are preferentially located at the interior pore surfaces.[40] In Figure 4, the O 1s, Zr 3d, and Si 2p core-level spectra for the sample

Table 1. Elemental analysis and structural parameters of ZrPMOs synthesized from different pathways.

| Si/Zr (gel) | Si/Zr ICP | XPS (solid) | Surface area[a] [$m^2 g^{-1}$] | Pore volume[b] [$cm^3 g^{-1}$] | Pore size[c] [nm] | Micropore volume[d] [$cm^3 g^{-1}$] |
|---|---|---|---|---|---|---|
| 100 | 106.4 | –[h] | 740 | 0.83 | 8.5 | 0.14 |
| 50 | 54.5 | 107.5 | 770 | 0.86 | 7.3 | 0.15 |
| 20 | 22.8 | 46.9 | 772 | 0.81 | 7.0 | 0.18 |
| 10 | 12.6 | 25.4 | 1048 | 1.19 | 5.9 | 0.17 |
| 10[e] | 21.5 | –[h] | 475 | 0.50 | 5.7 | 0.13 |
| 10[f] | 35.8 | –[h] | 707 | 0.48 | 6.2 | 0.26 |
| 10[g] | 86.2 | –[h] | 635 | 0.64 | 6.5 | 0.15 |

[a] Multipoint surface area calculated at relative pressure of $P/P_0$ = 0.05–0.25. [b] Total pore volume determined by the $N_2$ amount adsorbed at the highest $P/P_0$ (0.99). [c] Calculated by the conventional BJH method. [d] Calculated by the *t*-plot method with the use of experimental points at a relative pressure of $P/P_0$ = 0.10–0.20. [e] Synthesized by using 0.2 M HCl. [f] Synthesized by using 0.4 M HCl. [g] Synthesized by using and 1.0 M HCl. [h] Not determined.

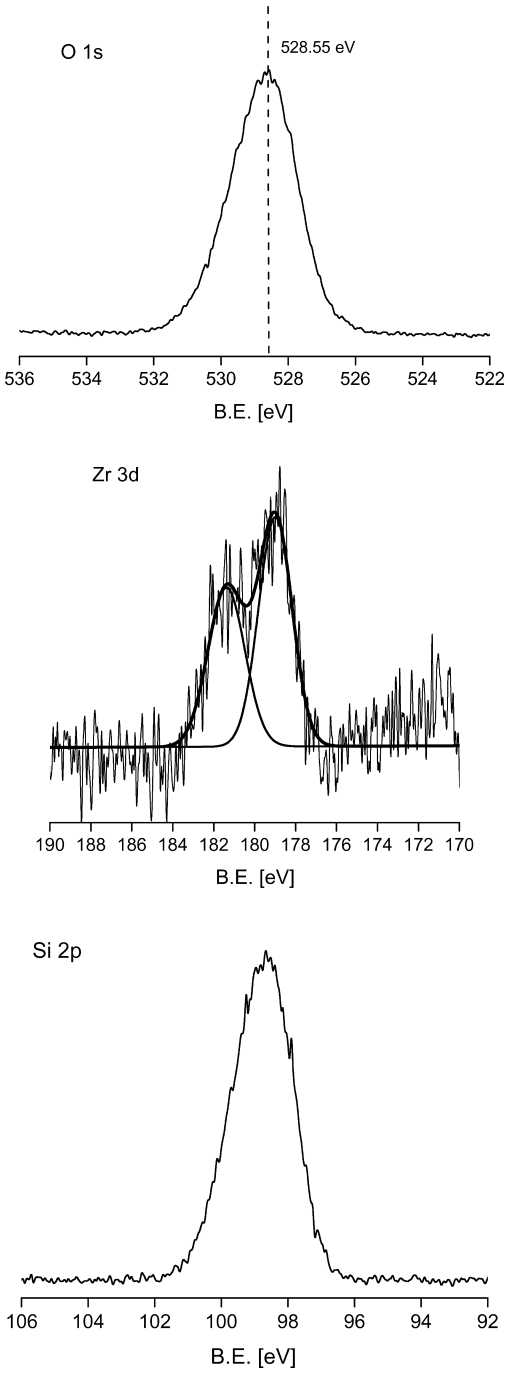


Figure 4. O 1s, Zr 3d, and Si 2p core-level spectra for the sample synthesized by using a $ZrOCl_2$–NaCl combination with Si/Zr = 10.

  

synthesized by using the salt pair with Si/Zr = 10 are presented as an example. The binding energy (BE) of O 1s (528.55 eV) was 1.65 eV lower than that given by oxygen in $ZrO_2$ (530.2 eV), and the binding energy of Zr 3d (179.1 eV) in this PMO material was also distinctly lower than that in $ZrO_2$ (181.9 eV). This significant shift indicated that no segregated oxide phase of zirconium was present,[40,41] which clearly supports the incorporation of zirconium into the hybrid framework. It should be noted, however, that the BE values for O 1s, Zr 3d, and Si 2p (98.65 eV) of this sample is considerably lower than that of the Zr-incorporated inorganic frameworks reported before,[40,41] which may be associated with the unique hybrid character of this PMO material. To the best of our knowledge, this is the first example of a preparation of highly ordered SBA-15-type ZrPMO materials with tunable framework zirconium content by the addition of inorganic salts and under such mild synthetic conditions.

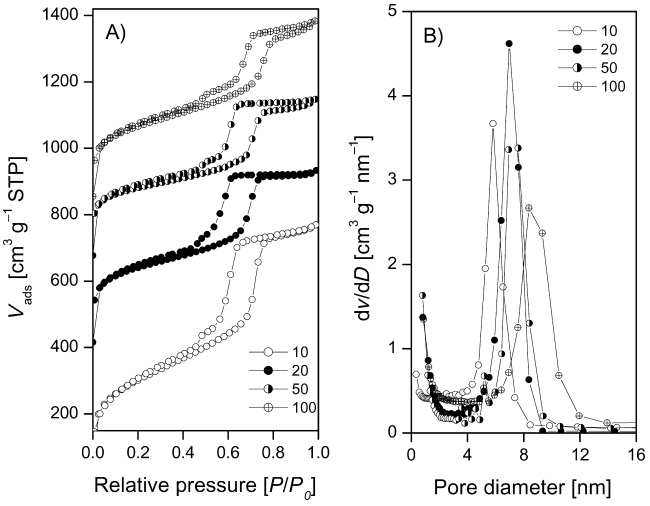


Figure 5. (A) Nitrogen adsorption isotherms and (B) BJH pore-size distributions of ZrPMO materials prepared by using the $ZrOCl_2$–NaCl combination with various Si/Zr molar ratios (as shown inset in the figures).

## Physical Properties

Figure 5 shows the nitrogen adsorption isotherms of the typical ZrPMO materials synthesized with different Si/Zr ratios by the $ZrOCl_2$–NaCl-assisted pathway. All samples exhibit a high degree of structural ordering, as indicated by the distinct capillary condensation step of the respective adsorption isotherm. This strongly suggests the presence of uniform cylindrical pores in these materials, in accordance with the 2D hexagonal pore structures revealed by the SAXS analysis and those reported results for SBA-15-like PMO or siliceous materials prepared under strongly acidic conditions.[7,34,42] Correspondingly, the pore-size distributions calculated from the adsorption branch clearly display a uniform pore structure for all samples (Figure 5B). The specific structural parameters derived from this sorption analysis such as total pore volumes, micropore volumes, pore sizes, and BET surface areas are summarized in Table 1. Noticeably, all ZrPMOs possess the typical structural properties of SBA-15-type materials such as large surface area and pore volume and a considerable amount of micropores,[34,42] and these textural features are comparable to those excellent SBA-15-like PMO or silica materials prepared from other synthesis systems.[7,34] Besides, it is interesting to note that a distinct relationship between the structural properties and preparation conditions can be drawn among these samples, that is, the specific surface areas and pore sizes clearly decrease and increase, respectively, with the Si/Zr ratios. All of these parameters indicate that the structural ordering, textural properties, and the incorporation of zirconium into the ZrPMO materials can be easily achieved by using different Si/Zr ratios by the synthesis pathway.

Consistent with the results of the SAXS and the physisorption measurements, respectively, the transmission electron microscopy (TEM) images of the representative samples viewed along different directions show well-ordered hexagonal arrays of 2D mesoporous channels (Figure 6), which further confirms that these samples are of *p6mm* hexagonal structure. Actually, no distinct difference can be found between this observation and that for P123-templated PMOs synthesized under various conditions such as such salt-assisted acidic synthesis[7,37] or the true-liquid-crystal-templating (TLCT) approach,[43] which strongly indicates the outstanding promoting effects of the salt pair in this synthetic system though the zirconium salt amount is very small; the function of both salts is entirely similar to that of reported Na(K)Cl/HCl combinations used for the synthesis of highly ordered mesostructures templated by block copolymers.[7,35,44,45]

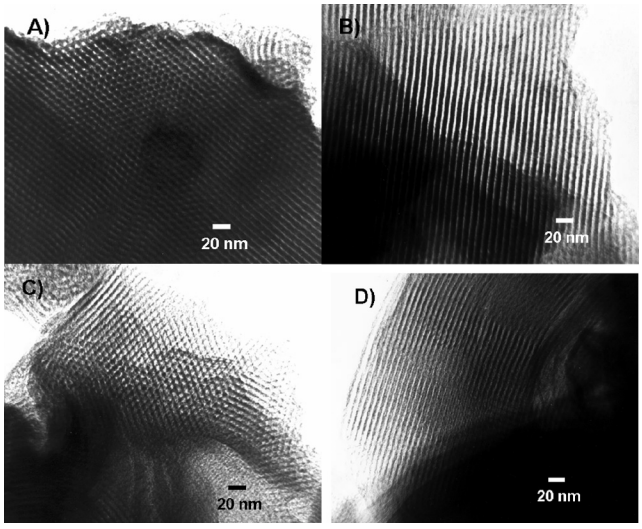


Figure 6. TEM micrographs of the samples synthesized by using the $ZrOCl_2$–NaCl pair with Si/Zr = 10 (A, B) and 100 (C, D).

The representative scanning electron microscopy (SEM) images for the ZrPMO materials synthesized with different Si/Zr ratios are shown in Figure S1 (Supporting Information). Clearly, no characteristic morphologies can be

  

found for all samples and irregular particles or aggregates are dominant through all the images, even though the particle/cluster size looks like it decreases with increasing Si/Zr ratios. Noticeably, these results are vastly different from those reported for SBA-15-type materials prepared under strongly acidic conditions, as described by Zhao et al., where wheat-like fibers composed of short rod-like particles were commonly observed.[34,42] This may be closely associated with the different preparation conditions (e.g. acidity, temperature, shear flow, ionic strength, etc.), which can exert a great impact on the hydrolysis and condensation kinetics of silica sources and therefore the morphological properties of the final mesophases.[34,46]

As far as this synthetic system is concerned, however, possibly there is no favorable orientation growth effect during the assembly process because of the fairly mild synthetic conditions. Under such conditions, the sol–gel kinetics of the organosilica precursor are so slow that the induction time for precipitation is too long to have a favorable effect on the macroscopic morphologies, even though this synthetic system is enough for the formation of ordered mesoporous frameworks. Actually, another observation directly confirmed the mildness of this synthesis system, that is, only less-ordered materials were obtained without stirring during the assembly process (see Figure S2); meanwhile, no distinct morphological variation was observed between both samples obtained with or without stirring during the synthesis (Figure S3). This result indicates that the shear flow is of great importance for the formation of highly ordered ZrPMO materials in this system due to the mild synthetic conditions, which is greatly different from the earlier work carried out in strongly acidic solutions.[47]

### Framework Properties

The $^{13}C$ cross-polarization (CP) and $^{29}Si$ MAS NMR spectra were used to clarify the basic structural information in these ZrPMO samples prepared with different Si/Zr ratios from the $ZrOCl_2$–NaCl-assisted synthesis. Interestingly, it was indeed found that there were no distinct differences in the spectra results between these samples, which indicates that the ethylene-bridging groups were completely intact in all samples, even though their framework compositions were different due to the variable zirconium content (see Table 1). For specific examples, Figure 7 shows the $^{13}C$ and $^{29}Si$ NMR spectra of two representative ZrPMO samples synthesized with Si/Zr = 10 and 100, respectively. In the case of the $^{13}C$ CP NMR spectra, a prominent peak is observed at 4.8 ppm for all samples, which is attributed to the ethylene carbon atoms covalently linked to the Si atoms in the framework.[7,8,43] Besides this, another three weak peaks at $\delta$ = 17.6, 57.8, and 70.1 ppm for the extracted samples can be assigned to the tiny amount of ethoxy ($-OC_2H_5$) groups exchanged during the extraction process and residual copolymer surfactant, respectively. However, in comparison with the sample prepared with Si/Zr = 100, a distinct peak due to the residual P123 is observed for the sample with a lower Si/Zr ratio of 10, though a similar extraction process was used for both samples. This result might be attributed to the presence of a relatively large amount of zirconium ions in the framework, which results in surfactant molecules that are more difficult to remove even under the identical extraction conditions.[38]

In addition, the $^{29}Si$ MAS NMR spectra of all samples exhibit two distinct signals at –56.5 and –64.0 ppm, which are attributable to the $T^2$ [C-*Si*(OH)$(OSi)_2$] and $T^3$ [C-*Si*$(OSi)_3$] silica species, respectively. Another very weak signal at –48.7 ppm due to the $T^1$ [C-*Si*$(OH)_2$(OSi)] silica environment is also observed. The strong intensity for the $T^2$ and $T^3$ signals indicates the formation of relatively condensed organosilicate frameworks for these samples; actually, there is no apparent difference between these materials and those prepared under strongly acidic conditions.[7,43]

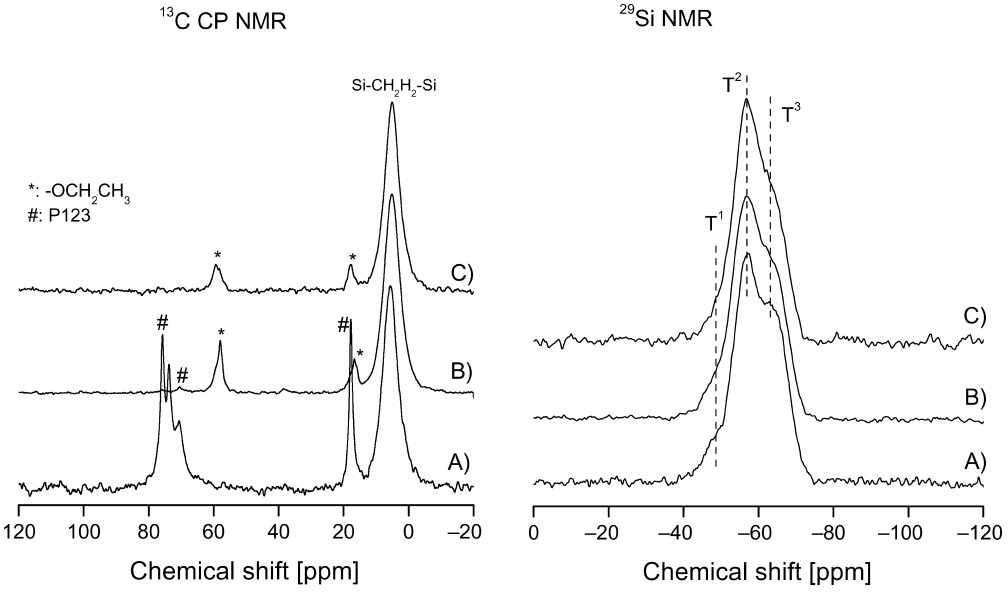


Figure 7. Solid-state $^{13}C$ CP and $^{29}Si$ MAS NMR spectra of the samples: (A) as-synthesized ZrPMO and (B) extracted ZrPMO obtained with Si/Zr = 10 by the salt-pair-assisted synthesis; (C) extracted ZrPMO prepared by using the similar method with Si/Zr = 100.

  

The absence of $SiO_4$ species such as $Q^3$ [*Si*(OH)$(OSi)_3$] and $Q^4$ [*Si*$(OSi)_4$], which produce signals between –90 and –120 ppm, indicates that no carbon–silicon bond cleavage of the BTME precursors occurred during this mild synthesis. These combined analyses clearly demonstrate that all of the Si atoms in these ZrPMO materials are bonded covalently to carbon atoms. It should be noted, however, that no significant changes in the $^{29}Si$ NMR spectra due to the different zirconium content incorporated into the framework can be seen for these samples. This is also an indication that the local environment of silica species in these hybrid materials is totally irregular in nature, which is similar to the previous results reported for Zr-incorporated SBA-15 silicas.[39,48]

Thermogravimetric analysis (TGA) conducted in flowing air and the derivative plots of as-synthesized and extracted ZrPMO synthesized with Si/Zr = 10 by the synthetic pathway are depicted in Figure 8. For both profiles, the weight loss below 120 °C is due to the removal of the physically adsorbed water or ethanol exchanged during the extraction process. A main weight loss (ca. 38%) in the range of 180–450 °C is observed for the as-synthesized one, which can be mainly assigned to the decomposition/combustion of the copolymer surfactant molecules.[39] After extraction, however, the weight loss (ca. 7%) observed in the same region appears too large to be attributed solely to the residual P123 surfactant, that is, there should be some contribution from the framework ethylene groups, which is consistent with the reported results[43,49] and the aforementioned $^{13}C$ CP NMR spectroscopic analysis that only a tiny amount of residual surfactant molecules were detected. However, it should be pointed out that the decompositions of the ethylene bridging groups is not only limited to this region, the weight loss over the range of 260–650 °C should be principally attributed to their removal under the present working conditions.[43]

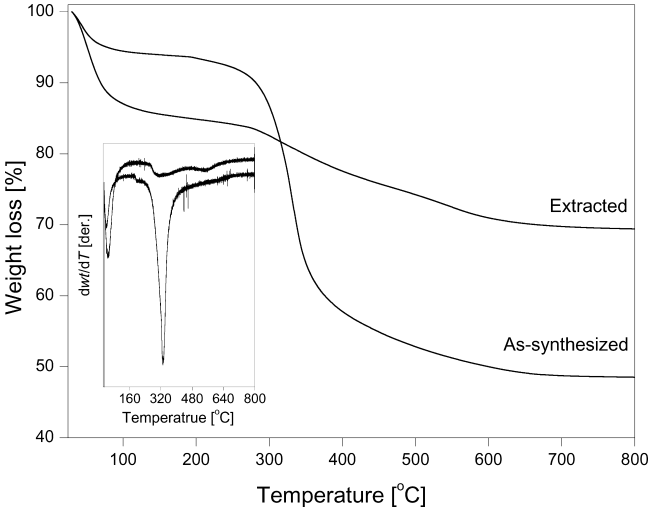


Figure 8. TG and DTG (inset) profiles of as-synthesized and solvent-extracted ZrPMO material prepared with Si/Zr = 10 by using this synthetic pathway.

**Plausible Mechanism**

Our results obtained by SAXS, $N_2$ sorption, XPS, TEM, and NMR spectroscopic techniques show that, even though no additional acid was added in the synthesis, highly ordered ZrPMO materials with a tunable zirconium content could be facilely prepared by using the $ZrOCl_2$/NaCl-assisted synthetic strategy by simply adjusting the amount of $ZrOCl_2$ in the synthesis gels. In practice, inorganic salts can play an important role in the synthesis of mesoporous materials especially for those nonionic surfactant-templating pathways, and recently a review article from Zhao et al. comprehensively detailed the effect of inorganic salts on the morphologies and structural properties of mesoporous silicates templated by nonionic surfactants.[35]

As far as the triblock copolymer-templating system (P123, F127, etc) is concerned, however, in most cases the inorganic additives are only nonhydrolyzable salts like sodium or potassium species, and the syntheses were still carried out under strongly acidic conditions.[7,44] In contrast, a combination of both "nonhydrolyzable" and "hydrolyzable" salts such as NaCl and $ZrOCl_2$ was used in this study under acid-free conditions. This synthetic pathway has never been reported for P123-templated PMOs, even though the NaCl/KCl-assisted acidic pathways have been frequently employed for the preparation of large-pore PMO materials.[7,37,45] It is well-established that both salts can respectively act as a well-understood micelle-promoting agent[35,44] (lower the critical micelle concentration and temperature of copolymer surfactant) and "catalyst"[39,50] for the hydrolysis and condensation of the silica precursors that were promoted by the self-generated acidity from the hydrolysis of inorganic $ZrOCl_2$. Indeed, the self-adjusted acidity, even though the zirconium salt amount (atomic ratio Si/Zr $\geq$ 10) added in the reaction gels is very small, is enough for the sol–gel processing of the bridged organosilanes due to their easier hydrolysis and condensation features in comparison with the conventional silica sources like tetraethoxysilane (TEOS) or tetramethoxysilane (TMOS).[51] Under such mild synthetic conditions, the induction time for precipitation is reasonably longer than that of the synthesis carried out under strongly acidic conditions, as described before, which might be responsible for the featureless morphologies of the final SBA-15-like ZrPMO products, even though their well-ordered framework channels could be easily assembled in this mild environment. As a matter of fact, this formation mechanism in nature is somewhat similar to the reported "acid–base pair" concept for those mesoporous nonsiliceous materials templated by copolymer surfactants, in which the appropriate acidity self-generated from the inorganic precursors is a key factor for the whole synthesis.[52,53] Likewise, in this work the organosilica precursor and $ZrOCl_2$ can be considered the so-called "base" and "acid", respectively. It is proposed that the hydrolyzed zirconyl cations may take the place of protons and adhere to either the hydrophilic side of the polymer micelle or the silanol group to form cationic species, which participate in the self-assembly process. Therefore, zirconium ions can be

  

effectively incorporated into the organosilicate frameworks due to the easiness of Zr–O–Si formation in this mild environment.[39,42] During this process, the presence of NaCl, a known micelle-promoting agent for copolymer P123, can change the ionic strength of the synthesis gels and favorably facilitate the formation of ordered ZrPMO materials, which has no direct interaction with the species involved in the self-assembly of the micelle and organosilica precursor.[39,46] Both salts have been found to be essential for the synthesis of highly ordered ZrPMO materials with large pore diameters.

## Conclusions

A new synthetic pathway was developed to incorporate zirconium ions into SBA-15-type PMO materials with excellent mesostructural ordering and tunable zirconium content by simply adjusting the $ZrOCl_2$ amount of the $ZrOCl_2$–NaCl salt combination, which was used as the promoting agent through the synthetic process and thus no additional mineral acids was necessary. A simple "neutralization" concept based on the chemical properties of the components of this synthesis system was discussed, in which the organosilica precursor and hydrolyzable $ZrOCl_2$ salt can be considered as the "base" and "acid", respectively. With this mechanism, the acidity self-generated by the zirconium salt is of great importance for the hydrolysis of the organosilica source. Simultaneously, the addition of NaCl can effectively enhance the interaction between the copolymer micelles and hydrolyzed species and facilitate the assembly of well-ordered ZrPMO materials. In comparison with those studies conducted under strongly acid conditions, this synthetic method is environmentally friendly and efficient in incorporating zirconium ions into the framework of the hybrid mesoporous materials. Actually, this synthetic pathway can also be applied to the preparation of other heteroatom-containing PMO materials, a series of Al-, Sn-, Fe-, and Cr-incorporated SBA-15-type mesostructures have been successfully prepared by using the corresponding inorganic chloride salts and will be reported in the near future.

## Experimental Section

**Chemicals:** All chemicals [zirconyl chloride octahydrate ($ZrOCl_2{\cdot}8H_2O, \geq 99\%$)] used as a zirconium source for the synthesis of zirconium-functionalized hybrid materials, triblock copolymer surfactant (Pluronic 123, molecular weight = 5800, $EO_{20}$-$PO_{70}EO_{20}$), and bis(trimethoxysilyl)ethane [$(CH_3O)_3SiCH_2CH_2Si(OCH_3)_3$, BTME, 96%] were purchased from Aldrich-Sigma Chemical Inc. All chemicals were used as received without further purification. Millipore water was used in all experiments.

**Synthesis of ZrPMO Materials:** Highly ordered ethylene-bridged ZrPMO materials can be successfully synthesized from BTME by using a $ZrOCl_2$–NaCl salt combination as the promoting agent for the assembly process, and there is no requirement for additional mineral acids. In a typical synthesis, P123 (1.5 g) and a predetermined amount of $ZrOCl_2{\cdot}8H_2O$ and NaCl were dissolved in deionized water (50 g) and stirred for 4 h at 40 °C. Then, BTME (1.96 mL) was added to the solution and stirred for 24 h at the same temperature, which was taken as the reaction temperature in the following text. The molar compositions of the synthesis are BTME/P123/$H_2O$/NaCl/$ZrOCl_2{\cdot}8H_2O$ = 1:0.034:400:0–8:0–0.4. The mother solution along with the precipitate was then transferred to an autoclave and hydrothermally treated for 48 h at 80 °C. The ZrPMO materials were finally obtained after filtration and two times extraction with HCl acidified ethanol (v/v, 3:100) at 60 °C for 6 h to remove the template.

**Characterization:** Small-angle X-ray scattering (SAXS) measurements were performed by using a synchrotron X-ray source of Pohang Accelerator Laboratory (PAL, Korea): Co-$K_\alpha$ ($\lambda$ = 1.608 Å) radiation with an energy range of 4–16 keV. Transmission electron microscopy (TEM) images were obtained with a JEOL2010 electron microscope with an acceleration voltage of 200 kV. Scanning electron microscopy (SEM) images were recorded with a JEOL 6400 microscope operating at 20 kV. Nitrogen adsorption isotherms were obtained with a Quantachrome's Quadrasorb SI analyzer at –196 °C. Before the measurements, the samples were degassed at 120 °C for 12 h in vacuo. The Brumauer–Emmett–Teller (BET) surface area was calculated by using experimental points at a relative pressure of $P/P_0$ = 0.05–0.25. The total pore volume was calculated by the $N_2$ amount adsorbed at the highest $P/P_0$ for each sample ($P/P_0$ = 0.99). The pore-size distribution was calculated by the conventional Barrett-Joyner-Halenda (BJH) method. The micropore area and volume were calculated by the *t*-plot method by using experimental points at a relative pressure of $P/P_0$ = 0.10–0.20. $^{13}C$ cross polarization (CP) and $^{29}Si$ MAS NMR spectra were obtained with a Bruker DSX400 spectrometer at room temperature with a 4 mm zirconia rotor spinning at 6 kHz (resonance frequencies of 79.5 and 100.6 MHz for $^{29}Si$ and $^{13}C$ CPMAS NMR, respectively; 90° pulse width of 5 μs, contact time 2 ms, recycle delay 3 s for both $^{29}Si$ and $^{13}C$ CP MAS NMR). Thermogravimetric analysis (TGA) was performed with a Perkin–Elmer Pyris Diamond TG instrument at a heating rate of 10 °C min$^{-1}$ in air. The zirconium content of the prepared ZrPMO materials was determined by ICP-Atomic Emission Spectroscopy (ICP-AES) by using a Plasma 400 (Perkin–Elmer) spectrometer equipped with Cetac6000AT+ ultrasonic nebulizer. To study the surface elements of the materials in their existing state, X-ray photoelectron spectroscopy (XPS) measurements were carried out with a PHI-1600ESCA System XPS spectrometer (Perkin–Elmer, USA) by using nonmonochromatic Mg-$K_\alpha$ radiation, operated at 15 kV and under $10^{-7}$ Pa pressure with photoelectron energy set at 1254 eV. The elements on the surface were quantified by using the peak areas.

**Supporting Information** (see footnote on the first page of this article): SEM images of the ZrPMO samples synthesized by using $ZrOCl_2$–NaCl with different Si/Zr molar ratios, SAXS patterns and SEM images of the samples synthesized.

## Acknowledgments

This work was financially supported by the Korea Science and Engineering Foundation (KOSEF) through the National Research Laboratory Program funded by the Ministry of Science and Technology, MOST (MOST; M10300000369-06J0000-36910), the SRC/ERC Program of MOST/KOSEF (R11-2000-070-080020), and the Brain Korea 21 Project. SAXS measurements at Pohang Accelerator Laboratory, Korea, are acknowledged.

  

[1] S. Inagaki, S. Guan, Y. Fukushima, T. Ohsuna, O. Terasaki, *J. Am. Chem. Soc.* **1999**, *121*, 9611–9614.
[2] B. J. Melde, B. T. Holland, C. F. Balandford, A. Stein, *Chem. Mater.* **1999**, *11*, 3302–3308.
[3] T. Asefa, M. J. MacLachlan, N. Coombs, G. A. Ozin, *Nature* **1999**, *402*, 867–871.
[4] F. Hoffmann, M. Cornelius, J. Morell, M. Fröba, *Angew. Chem. Int. Ed.* **2006**, *45*, 3216–3251.
[5] T. Asefa, M. J. MacLachlan, H. Grondey, N. Coombs, G. A. Ozin, *Angew. Chem. Int. Ed.* **2000**, *39*, 1808–1811.
[6] A. Sayari, S. Hamoudi, Y. Yang, I. L. Moudrskovski, J. R. Ripmeester, *Chem. Mater.* **2000**, *12*, 3857–3863.
[7] W. P. Guo, J. Y. Park, M. O. Oh, H. W. Jeong, W. J. Cho, I. Kim, C. S. Ha, *Chem. Mater.* **2003**, *15*, 2295–2298.
[8] X. Y. Bao, X. S. Zhao, X. Li, P. A. Chia, J. Li, *J. Phys. Chem. B* **2004**, *108*, 4684–4689.
[9] Y. Xia, W. Wang, R. Mokaya, *J. Am. Chem. Soc.* **2005**, *127*, 790–798.
[10] J. Morell, G. Wolter, M. Fröba, *Chem. Mater.* **2005**, *17*, 804–808.
[11] J. Liu, Q. H. Yang, L. Zhang, D. Jiang, X. Shi, H. Q. Yang, H. Zhong, C. Li, *Adv. Funct. Mater.* **2007**, *17*, 569–576.
[12] S. Inagaki, S. Guan, T. Ohsuna, O. Terasaki, *Nature* **2002**, *416*, 314–317.
[13] A. Sayari, W. Wang, *J. Am. Chem. Soc.* **2005**, *127*, 12194–12195.
[14] M. P. Kapoor, Q. H. Yang, S. Inagaki, *J. Am. Chem. Soc.* **2002**, *124*, 15176–15177.
[15] O. Olkhovyk, M. Jaroniec, *J. Am. Chem. Soc.* **2005**, *127*, 60–61.
[16] O. Olkhovyk, M. Jaroniec, *Ind. Eng. Chem. Res.* **2007**, *46*, 1745–1751.
[17] T. Asefa, M. Kruk, M. J. MacLachlan, N. Coombos, H. Gronden, M. Jaroniec, G. A. Ozin, *J. Am. Chem. Soc.* **2001**, *123*, 8520–8530.
[18] Q. H. Yang, J. Liu, J. Yang, *J. Catal.* **2004**, *228*, 265–272.
[19] M. A. Wahab, I. Imae, Y. Kawakami, C. S. Ha, *Chem. Mater.* **2005**, *17*, 2165–2174.
[20] D. M. Jiang, Q. H. Yang, J. Yang, L. Zhang, G. R. Zhu, W. Su, C. Li, *Chem. Mater.* **2005**, *17*, 6154–6160.
[21] J. Morell, M. Güngerich, G. Wolter, J. Jiao, M. Hunger, P. J. Klar, M. Fröba, *J. Mater. Chem.* **2006**, *16*, 2809–2818.
[22] C. Baleizao, B. Gigante, D. Das, M. Alvaro, H. Garcia, A. Corma, *Chem. Commun.* **2003**, 1860–1861.
[23] A. Corma, D. Das, H. Garcia, A. Leyva, *J. Catal.* **2005**, *229*, 322–331.
[24] Q. Yang, Y. Li, L. Zhang, J. Yang, C. Li, *J. Phys. Chem. B* **2004**, *108*, 7934–7937.
[25] B. J. Hughes, J. B. Guilbaud, M. Allix, Y. Z. Khimyak, *J. Mater. Chem.* **2005**, *15*, 4728–4733.
[26] W. P. Guo, X. S. Zhao, *Microporous Mesoporous Mater.* **2005**, *85*, 32–38.
[27] M. P. Kapoor, A. Bhaumik, S. Inagaki, K. Kuraoka, T. Yazawa, *J. Mater. Chem.* **2002**, *12*, 3078–3083.
[28] M. P. Kapoor, A. Sinha, S. Seelan, S. Inagaki, S. Taubota, H. Yoshida, M. Haruta, *Chem. Commun.* **2002**, 2902–2903.
[29] A. Bhaumik, M. P. Kapoor, S. Inagaki, *Chem. Commun.* **2003**, 470–471.
[30] W. Cho, J. W. Park, C. S. Ha, *Mater. Lett.* **2004**, *58*, 3551–3554.
[31] S. Shylesh, A. P. Singh, *Microporous Mesoporous Mater.* **2006**, *94*, 127–138.
[32] S. Shylesh, Ch. Srilakshmi, A. P. Singh, B. G. Anderson, *Microporous Mesoporous Mater.* **2007**, *99*, 334–344.
[33] J. A. Melero, J. Eglesias, J. M. Arsuaga, J. Sainz-pardo, P. de Frutos, S. Blazquez, *J. Mater. Chem.* **2007**, *17*, 377–385.
[34] D. Y. Zhao, J. L. Feng, Q. S. Huo, N. Melosh, G. H. Fredrickson, B. F. Chmelka, G. D. Stucky, *Science* **1998**, *279*, 548–552.
[35] Y. Wan, Y. F. Shi, D. Y. Zhao, *Chem. Commun.* **2007**, 897–926.
[36] X. G. Cui, W. C. Zin, C. S. Ha, *Mater. Lett.* **2005**, *18*, 2257–2261.
[37] S. Z. Qiao, C. Z. Yu, Q. H. Hu, Y. G. Jin, X. S. Zhao, G. Q. Lu, *Microporous Mesoporous Mater.* **2006**, *91*, 59–69.
[38] S. Shylesh, P. P. Samuel, A. P. Singh, *Microporous Mesoporous Mater.* **2007**, *100*, 250–258.
[39] S. Y. Chen, L. Y. Jang, S. Cheng, *Chem. Mater.* **2004**, *16*, 4174–4180.
[40] J. M. Liu, S. J. Liao, G. D. Jiang, X. L. Zhang, L. Petrik, *Microporous Mesoporous Mater.* **2006**, *95*, 306–311.
[41] A. Infantes Molina, J. Mérida Robles, P. Maireles Torres, E. Finocchio, G. Busca, E. Rodríguez Castellón, J. L. G. Fierro, A. Jiménez López, *Microporous Mesoporous Mater.* **2004**, *75*, 23–32.
[42] M. Selvaraj, S. Kawi, *Chem. Mater.* **2007**, *19*, 509–519.
[43] H. Zhu, D. J. Jones, J. Zajac, J. Rozière, R. Dutartre, *Chem. Commun.* **2001**, 2568–2569.
[44] C. Z. Yu, B. Z. Tian, B. Fan, G. D. Stucky, D. Y. Zhao, *Chem. Commun.* **2001**, 2726–2727.
[45] X. F. Zhou, S. Z. Qiao, N. Hao, X. Wang, C. Z. Yu, L. Wang, D. Y. Zhao, G. Q. Lu, *Chem. Mater.* **2007**, *19*, 1870–1876.
[46] C. Z. Yu, J. Fan, B. Z. Tian, D. Y. Zhao, G. D. Stucky, *Adv. Mater.* **2002**, *14*, 1742–1745.
[47] A. Sayari, B. H. Han, Y. Yang, *J. Am. Chem. Soc.* **2004**, *126*, 14348–14349.
[48] F. X. Li, F. Yu, Y. Li, R. Li, K. Xie, *Microporous Mesoporous Mater.* **2007**, *101*, 250–255.
[49] R. M. Grudzien, B. E. Grabicka, S. Pinkus, M. Jaroniec, *Chem. Mater.* **2006**, *18*, 1722–1725.
[50] P. Shah, A. V. Ramaswamy, K. Lazar, V. Ramaswamy, *Microporous Mesoporous Mater.* **2007**, *100*, 210–226.
[51] X. Y. Bao, X. S. Zhao, S. Z. Qiao, S. K. Bhatia, *J. Phys. Chem. B* **2004**, *108*, 16441–16450.
[52] B. Z. Tian, X. Y. Liu, B. Tu, C. Z. Yu, J. Fan, L. M. Wang, S. H. Xie, G. D. Stucky, D. Y. Zhao, *Nat. Mater.* **2003**, *2*, 159–163.
[53] Y. Wan, H. F. Yang, D. Y. Zhao, *Acc. Chem. Res.* **2006**, *39*, 423–432.

Received: July 23, 2007
Published Online: October 17, 2007

  